

Neutron Electric Dipole Moment and Lattice QCD Calculations

Keh-Fei Liu^{a,b,*}

^a*Department of Physics and Astronomy, University of Kentucky, Lexington, KY 40506, USA*

^b*Nuclear Science Division, Lawrence Berkeley National Lab, Berkeley, CA 94720, USA*

E-mail: liu@g.uky.edu

We review the lattice QCD calculations of the neutron and proton electric dipole moments (EDMs) and the CP-violating πNN coupling constant due to the θ term in the last few years. We also discuss the progress towards nucleon EDM calculations with the Weinberg operator, and the quark chromoelectric dipole moment operator.

*The 42nd International Symposium on Lattice Field Theory (LATTICE2025)
2-8 November 2025
Tata Institute of Fundamental Research, Mumbai, India*

*Speaker

1. Introduction

There are two sources of CP violation in the standard model that contribute to the neutron electric dipole moment (nEDM). One is the CKM matrix in the weak interaction, which induces an EDM of the quarks at the two-loop order [1, 2] involving heavy quarks. The recent results from the CKM matrix calculation of nEDM d_n and proton EDM (pEDM) d_p are $1 \times 10^{-32} e \cdot \text{cm} < \{|d_n(\text{CKM})|, |d_p(\text{CKM})|\} < 6 \times 10^{-32} e \cdot \text{cm}$ [3]. This range is 5 to 6 orders of magnitude smaller than the current upper limit on the nEDM. Thus, nEDM experiments have a good discovery potential for BSM physics.

The second source is the θ -term in QCD, represented by the topological charge operator $-\bar{\theta} \frac{g^2}{32\pi^2} G_{\mu\nu}^a \tilde{G}_{\alpha\beta}^a$. The EDM induced by the CKM matrix is suppressed due to the flavor non-diagonal nature of quark flavor-mixing. The topological charge term is the only four-dimensional flavor-diagonal operator that can produce an EDM. If this is the sole contribution to the EDM, the current experimental limit on EDM implies that $\bar{\theta} < 10^{-10}$ based on chiral symmetry considerations of a pion loop contribution [4, 5]. In contrast to the CKM matrix where δ_{CKM} is of order unity, this small $\bar{\theta}$ is known as the strong CP problem.

One proposed solution to address the strong CP problem is the introduction of the axion - a pseudo-Goldstone boson - via the Peccei-Quinn mechanism [6]. In this framework, $\bar{\theta}$ becomes a dynamical field with a potential minimized at $\bar{\theta} = 0$. The smallness of $\bar{\theta}$ can be understood as being dynamically relaxed [6–9], though generally not to exactly zero, due to effects that violate the Peccei-Quinn symmetry [10–13]. Another possibility is that there are BSM interactions responsible for CP violation, which can be classified as higher dimensional operators in effective theories. Some of these operators can mix with the four-dimensional topological term. The smallness of $\bar{\theta}$ would then reflect the large scale of BSM physics.

While BAU and nEDM may require new beyond Standard Model (BSM) physics, relating nuclear and atomic EDMs to the high-energy CP violation mechanism will necessitate hadronic and nuclear inputs. Below the BSM scale, flavor-diagonal CP violation can be described by extending the Standard Model (SM) Lagrangian with gauge-invariant higher-dimensional operators, leading to a standard model effective field theory (SMEFT) [14–16]. A list of operators relevant to CP violation can be found in [17]. To address hadron and nuclear systems below the electroweak scale, heavy SM degrees of freedom, such as W and Z bosons and the Higgs, can be integrated out by matching the SMEFT Lagrangian to a low-energy effective field theory (LEFT) [18, 19]. The complete one-loop matching calculation has been carried out [20]. A subset of operators relevant to EDM, estimated to have dominant contributions [21], include the quark EDM (qEDM), the quark chromo-EDM (qcEDM), the gluon chromo-EDM (gcEDM) — known as the Weinberg operator [22] — and the four-fermion operators.

The discovery of an electric dipole moment (EDM) in any single system — be it a hadron, a lepton or a molecule — would represent a significant breakthrough and paradigm-shift. However, it would not be sufficient to definitely identify the source or discriminate among different BSM models. It is necessary to bound EDMs in complementary systems to identify the characteristic features of CP violation at low-energies and establish a connection to the underlying BSM origin. One crucial ingredient in this process is having reliable theoretical estimates of the relevant matrix elements for the aforementioned CP-violating operators. This is where lattice QCD calculations

come into play.

Over the last five decades, lattice QCD calculations based on the Euclidean path-integral formulation of QCD on a discrete space-time lattice [23] have developed into a powerful tool for *ab initio* calculations of strong-interaction physics. It is presently the only theoretical approach to solving QCD with controlled systematic errors. Many of the recent lattice ensembles have reached the physical pion mass, allowing for systematic errors in continuum and infinite volume extrapolations to be quantified, controlled, and improved.

Lattice fermion formulations that accommodate chiral symmetry have been developed over the last three decades, including domain-wall fermions (DWF) [24, 25], overlap fermions [26], and fixed-point fermions [27]. In this review, we will discuss the progress on lattice calculations of the θ term, the qEDM, the qcEDM, and the Weinberg operator. Previous reviews on the subject has been given in [28, 29]. This review serves as an update on the latest lattice results, particularly concerning the θ term and the CP-violating πNN coupling. We will not discuss the four-fermion operators as there are currently no lattice calculations for these operators.

2. QCD θ Term

The QCD action in Euclidean space with the θ term is given by:

$$S_{QCD+\bar{\theta}}^E = S_{QCD}^E - i\bar{\theta}Q, \quad (1)$$

where $Q = \frac{g^2}{32\pi^2} G_{\mu\nu}^a \tilde{G}_{\mu\nu}^a$ is the topological charge. Since the θ term is imaginary, the usual probability based Monte Carlo approach encounters a sign problem. However, considering that $\bar{\theta} \ll 1$, one can Taylor expand in $\bar{\theta}$ to calculate observables in the presence of Q :

$$\langle O(\psi, \bar{\psi}, U) \rangle_{\bar{\theta}} \longrightarrow \langle O \rangle_{\bar{\theta}=0} - i\bar{\theta} \langle O Q \rangle_{\bar{\theta}=0} + O(\bar{\theta}^2). \quad (2)$$

Thus, to first order in $\bar{\theta}$, one can calculate $\langle O Q \rangle_{\bar{\theta}=0}$. We shall use Euclidean notation in the following text.

The common calculation of the neutron electric dipole moment (nEDM) is conducted through the vector form factor in the presence of the θ term in the action. In this case, the vector current form factor is given by [30]

$$\langle N(p') | J_{\mu}^{em} | N p \rangle_{\bar{\theta}} = \bar{u}_{p'} \Gamma_{\mu} u_p, \quad (3)$$

where

$$\Gamma_{\mu} = \gamma_{\mu} F_1(q^2) - \frac{\sigma_{\mu\nu} q_{\nu}}{2M_N} [F_2(q^2) - iF_3(q^2)\gamma_5] + \frac{F_A(q^2)}{m_N} (\not{q} q_{\mu} - q^2 \gamma_{\mu}) \gamma_5. \quad (4)$$

Here, $\sigma_{\mu\nu} = [\gamma_{\mu}, \gamma_{\nu}]/2i$, $F_3(q^2)$ is the electric dipole form factor, and $F_A(q^2)$ is the anapole form factor.

It has been noted [31, 32] that the linear $\bar{\theta}$ dependence comes in two places: one is the insertion of $-i\bar{\theta}Q$ in addition to the current J_{μ}^{em} , and the other is through the nucleon state, which acquires a CP-breaking phase. Specifically, the nucleon spinor in the $\bar{\theta}$ vacuum becomes: $u_{\bar{\theta}} = e^{i\bar{\theta}\alpha_5\gamma_5} u$, and $\bar{u}_{\bar{\theta}} = \bar{u} e^{i\bar{\theta}\alpha_5\gamma_5}$. It was shown [30] that the combinations

$$F_3(q^2) = \tilde{F}_3(q^2) + 2\alpha_5 \tilde{F}_2(q^2), \quad F_2(q^2) = \tilde{F}_2(q^2) - 2\alpha_5 \tilde{F}_3(q^2) \quad (5)$$

transform as an axial vector and vector, respectively. Thus, the electric dipole moment is given by:

$$d_N = \lim_{q^2 \rightarrow 0} \frac{F_3(q^2)}{2M_N} \quad (6)$$

where \tilde{F}_3 and \tilde{F}_2 are those calculated without considering the CP phase in the nucleon state. Previous lattice nEDM calculations [31, 33–36] did not take the $2\alpha\tilde{F}_2$ term into account. When it was included, the results were within one sigma of zero, indicating that no nEDM had been observed [30].

Furthermore, directly calculating with re-weighting of the total topological charge Q in the evaluation of the correlator $\langle OQ \rangle$ in Eq. (2) is not practical. The average $|Q|$ in an ensemble grows with \sqrt{V} , the square root of the volume, which induces large fluctuations and negatively affects the signal-to-noise ratio (SNR) as V increases. It has been found that considering the total Q as the sum of the local charge $q(x)$ (i.e., $Q = \int d^4x q(x)$) and summing a subset of q over limited time slices straddling the current time position reduces the error [35]. This is a consequence of cluster decomposition [37], and one can use this property to reduce variance through a cluster decomposition error reduction technique (CDER) [37], which we will discuss later.

New lattice efforts have been initiated [38–43]. One lattice calculation [39] used the clover fermions on a lattice with a spacing of $a = 0.0907$ fm and investigated three pion masses at 410, 568, and 699 MeV for chiral extrapolation. Additionally, it included three lattice spacings of 0.0684, 0.0936 and 0.1095 fm, with a pion mass around 680 MeV for continuum extrapolation. The authors employed gradient flow [44, 45] to define the local topological charge, which yields integer Q and does not require renormalization. They also adopted a cluster decomposition error reduction technique (CDER) for the time slices to reduce errors in both the two- and three-point functions. The results obtained were $d_n = -0.00152(71) \bar{\theta} e \cdot \text{fm}$ and $d_p = 0.0011(10) \bar{\theta} e \cdot \text{fm}$. The reported nucleon Schiff moments reported are $S_n = -0.10(43) \times 10^{-4} \bar{\theta} e \cdot \text{fm}$ and $S_p = 0.50(59) \times 10^{-4} \bar{\theta} e \cdot \text{fm}$.

Another calculation using $N_f = 2 + 1 + 1$ twisted mass and clover-improved fermion action was conducted by the Extended Twisted Mass Collaboration (ETMC) [40]. The lattice has a physical size of 5.13 fm with a spacing of approximately $a \simeq 0.08$ fm, and a pion mass at the physical value of 139 MeV. The fermion version was used for the topological charge operator Q . This formulation was found to be less noisy than that constructed from the gauge link variables, whether using gradient flow, link smearing, or cooling [46], and has smaller discretization errors. They obtained the nEDM value as $|d_n| = 0.0009(24) \bar{\theta} e \cdot \text{fm}$.

The Los Alamos group utilized the valence clover action on the $N_f = 2 + 1 + 1$ highly improved staggered quark (HISQ) gauge configurations for their nEDM calculation. They worked with nine ensembles featuring lattice spacings ranging from 0.0570 fm to 0.1207 fm and pion masses from the physical value of 135 MeV to 320 MeV [41]. The topological charge operator was obtained from the gradient flow and the $O(a)$ effects were considered due to the non-chiral valence quarks [47] and the fact that the vector current is not $O(a)$ improved. Their chiral extrapolation fits, which included chiral logarithms, yielded $d_n = -0.003(7)(20) \bar{\theta} e \cdot \text{fm}$ and $d_p = 0.024(10)(30) \bar{\theta} e \cdot \text{fm}$.

A recent calculation on the subject was carried out by the χ QCD collaboration [42]. They employed overlap fermions on $2 + 1$ -flavor domain-wall fermion (DWF) configurations on $24^3 \times 64$ lattices for three ensembles with sea pion masses at 339, 432, and 560 MeV. For each ensemble with a

different sea quark mass, they calculated 3 to 4 valence quark masses for partially quenched analyses. The local topological charge operator was defined with the overlap operator for consistency [48, 49]. Thanks to the chiral nature of both the valence overlap fermions and the sea DWF, they achieved results with smaller statistical errors: $d_n = -0.00148(14)(31) \bar{\theta} e \cdot \text{fm}$ and $d_p = 0.0038(11)(8) \bar{\theta} e \cdot \text{fm}$. We shall present some details of this calculation in the following. The results of these calculations are tabulated in Table 1 and plotted in Fig. 1.

Table 1: Summary of recent lattice calculations of the neutron electric dipole moment (nEDM) and proton electric dipole moment (pEDM) from the θ term, including the quark actions, lattice spacings, and pion masses.

Action (ref.)	a (fm)/ m_π (MeV)	d_n ($\bar{\theta} e \cdot \text{fm}$)	d_p ($\bar{\theta} e \cdot \text{fm}$)
Clover [39]	0.0907 / 410, 568, 699	-0.00152(71)	0.0011(10)
	0.0684, 0.0936, 0.1995 / ~ 680		
Twisted Mass [40]	0.08 / 139	0.0009(24)	-
Clover+HISQ [41]	0.0570 - 0.1207 / 135 - 320	- 0.003(7)(20)	0.024(10)(30)
Overlap+DWF [42]	0.0114 / 339, 432, 560	- 0.00148 (14) (31)	0.0038 (11) (8)

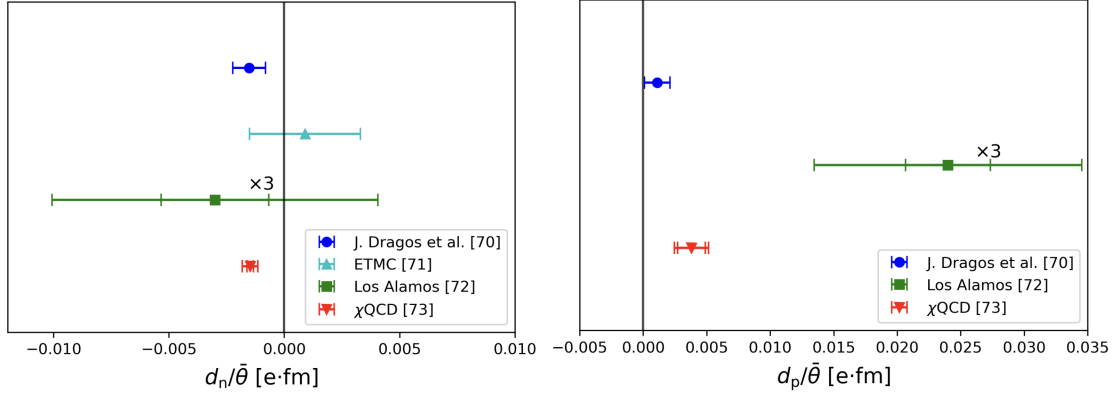


Figure 1: The lattice calculation results in Table 1 are plotted. The left and right panel is for nEDM and pEDM respectively. The legends give their reference numbers.

Other efforts calculating the nEDM from the θ term using Domain-Wall-Fermions (DWF) has also been attempted [38, 43]. A background field approach [43] with DWF has reported preliminary results for nEDM at two pion masses: $d_n / \bar{\theta}$ (340MeV) = $-0.0072(20)$, and $d_n / \bar{\theta}$ (420MeV) = $-0.0060(20)$.

2.1 Nucleon EDM and cluster decomposition error reduction (CDER)

We shall give some details of the calculation by the χ QCD collaboration with the overlap fermions [42]. The lattice F_3 form factors for the nEDM and pEDM are extracted from the three-

and two-point correlation functions

$$F_3(q^2) = \frac{2m}{E_f + m} \left\{ \frac{2E_f}{q_i} \frac{\text{Tr} [\Gamma_i C_3(V_\mu)^Q]}{\text{Tr} [\Gamma_e C_2]} - \alpha_5 G_E(q^2) \right\}, \quad (7)$$

where $G_E(q^2)$ is the electric form factor and α_5 is the CP phase of the nucleon in Eq. (??),

$$G_E(q^2) = \frac{2E_f}{E_f + m} \frac{\text{Tr} [\Gamma_e C_3(V_\mu)]}{\text{Tr} [\Gamma_e C_2]}, \quad \alpha_5 = \frac{\text{Tr} [\gamma_5 C_2^Q]}{2\text{Tr} [\Gamma_e C_2]}. \quad (8)$$

Here, V_μ is the EM current operator. $C_3(V_\mu)$ is the three-point correlator with nucleon interpolation fields at source and sink time positions of 0 and t_f , and the vector current insertion occurs at time t . The source, sink and current have momenta projections of \vec{p}_i, \vec{p}_f and \vec{q} , respectively, such that the momentum transfer is q^2 . $C_3(V_\mu)^Q$ is the $C_3(V_\mu)$ correlator with the topological charge Q insertion. C_2 and C_2^Q are the corresponding two-point functions with the same source and sink at 0 and t_f . $\Gamma_e = \frac{1+\gamma_4}{2}$ is the unpolarized spin projector, and $\Gamma_i = -i\gamma_5\gamma_i\Gamma_e$ is the polarized projector along the i direction. This formalism applies equally to both the neutron and the proton.

One often invokes the locality argument to justify that experiments conducted on Earth are not affected by events on the Moon. This stems from the cluster decomposition principle (CDP), which states that if color-singlet operators in a correlator are separated by a sufficient large space-like distance, the correlator will be zero. However, the disconnected insertion (DI) calculation of the three-point function, such as the calculation of nEDM with the θ term, encounters a noise issue due to the \sqrt{V} fluctuation. These problems were identified [37] as stemming from the fact that the variance of the disconnected insertion has a leading intermediate vacuum state insertion, causing the operator and the nucleon propagator in the disconnected insertion (DI) to fluctuate independently. This leads to a variance that is the product of their respective variances. In this case, the vacuum insertion is a constant, independent of t . This is why the noise remains constant over t in DI. In the case of the correlator $\text{Tr}(\gamma_5 C_2^Q)$, which is needed to obtain the CP phase α_5 in Eq. (8), one can consider Q as a sum of the local topological charge, i.e., $Q = \sum_x q(x)$, so that one can take the 4-D accumulated sum of $q(x)$ with a radius R away from the sink position using FFT. In the calculation of the CP phase α on a $48^3 \times 96$ DWF lattice (with $a = 0.114$ fm, $m_\pi = 139$ MeV) using overlap fermions for the valence quarks and $q(x) = \frac{1}{2} \text{Tr}_{cs}(\gamma_5 D_{ov}(x, x))$ reveals that the resulting signal saturates after $R \sim 16$. Since the signal falls off exponentially due to the CDP, there is no further signal after this point, yet the error continues to accumulate. This suggests that the sum should be truncated at R . Cutting off the sum of $q(x)$ at this radius results in a factor of ~ 3.6 times reduction in error compared to the case of reweighting with the total topological charge as in Eq. (8). This approach can increase the signal to noise ratio (SNR) by $\sqrt{V/V_R}$ where V_R is the volume with the radius R . This variance reduction technique, known as the cluster decomposition error reduction (CDER), has been applied to the disconnected insertion (DI) calculations with quark loops [50–53] and glue operators [42, 53, 54].

Besides applying CDER to the calculation of nEDM and pEDM to reduce errors from the DI of the topological charge [42], additional variance reduction arises from the chiral nature of overlap fermions. The anomalous Ward identity is preserved by the overlap fermion action and the $q(x)$ from the overlap Dirac operator. Consequently, the EDM at the chiral limit is zero on the lattice

at finite lattice spacing (This is not true with non-chiral fermions; in this case, one must first take the continuum limit to satisfy the AWI.) The results of the nEDM for three ensembles of the DFW configurations (see Table 1 for pion masses) are plotted in Fig. 2 as a function of m_π^2 . The left panel shows the unitary case where the valence and sea pion masses are matched. Since $d_{n/p}$ anchored at the chiral limit is zero, a chiral interpolation can be performed to reach the physical pion point, incorporating a chiral log in the fitting. The result $d_n = -0.00142(20)(29) \bar{\theta} e \cdot \text{fm}$ is obtained, with the total systematic uncertainty arising from excited-state contamination, the CDER cutoff, the Q^2 extrapolation and chiral interpolation.

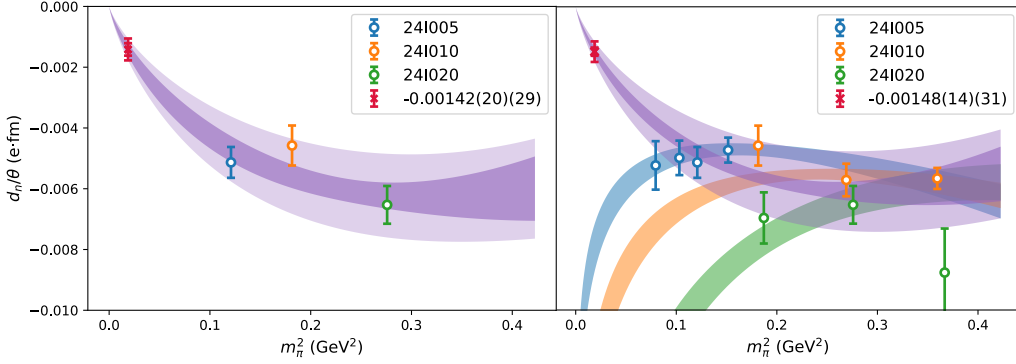


Figure 2: The neutron electric dipole moment as a function of m_π^2 is interpolated between the zero quark mass limit and three heavier pion masses. The left panel represents the unitary case, where the valence and sea quarks are the same. The right panel illustrates the case with 3 to 4 valence quarks for each sea quark ensemble in a partially quenched chiral perturbation interpolation. The red points indicate the values interpolated to the physical pion mass.

Results from the partially quenched cases, with several valence quark masses for each sea mass, are plotted in the right panel of Fig. 2. It is observed that the chiral behaviors of the sea and valence pions seem to diverge, moving in opposite directions as the pion mass decreases. This behavior was predicted in a partially quenched χ PT [55] calculation, which indicates that the terms linear in m_π^2 have different signs for the sea and the valence pions. Consequently, the following form was used in the chiral interpolation, including both the valence and sea contributions.

$$d_n = c_1 m_{\pi,s}^2 \log\left(\frac{m_{\pi,v}^2}{m_N^2}\right) + c_2 m_{\pi,s}^2 + c_3 (m_{\pi,v}^2 - m_{\pi,s}^2), \quad (9)$$

where $m_{\pi,v}$ and $m_{\pi,s}$ are the valence and sea pion masses, respectively. With additional partially quenched data, the nEDM is found to be $d_n = -0.00148(14)(31) \bar{\theta} e \cdot \text{fm}$, reflecting a 30% reduction in the statistical error compared to the unitary case. The 10-sigma result (statistical error) represents a significant improvement over the previous 2-sigma result [56]. This enhancement is primarily due to the combination of CDER, chiral fermion interpolation, and the inclusion of partially quenched data. The proton EDM is also obtained in the same calculation, yielding $d_p = 0.038(11)(8) \bar{\theta} e \cdot \text{fm}$.

A precise determination of d_n and d_p is important for systems that are sensitive to the iso-singlet combination $d_n + d_p$, where the one-loop chiral perturbation contributions almost cancel. This supports the notion that it is necessary to measure EDMs in various systems experimentally, as they might be sensitive to different sources of CP violation.

2.2 Chiral perturbation theory and CP-violating π NN coupling

The extraction of solid information on possible new sources of CP violation from EDM measurements involves dynamics across a wide variety of scales, from the new physics scale $\Lambda_{\mathcal{CP}}$ to the electroweak (EW) and QCD scales, down to the atomic scale. At the QCD scale, the interpretation of EDM experiments involving more than one nucleon additionally depends on CP-violating (CPV) nucleon-nucleon interactions. Heavy Baryon Chiral Perturbation Theory (HB χ PT) [57] has been extended to include parity and time reversal breaking Lagrangians. The chiral power counting predicts that these interactions mainly depend on one-pion-exchange contributions involving CP violating (CPV) pion-nucleon vertices [21, 58–60]. Calculations of the CPV pion-nucleon coupling constants are therefore as important as those of nucleon EDMs. The relevant CPV pion-nucleon coupling Lagrangian includes the following terms

$$\mathcal{L}_{\text{eff}}^{\mathcal{CP}} = \bar{g}_0 \bar{N} \boldsymbol{\tau} \cdot \boldsymbol{\pi} N + \bar{g}_1 \pi_0 N + \bar{g}_2 \pi_0 \boldsymbol{\tau}^3 N, \quad (10)$$

where the low-energy constants (LECs) \bar{g}_0 , \bar{g}_1 and \bar{g}_2 represent the iso-scalar, iso-vector, and iso-tensor CP-odd pion-nucleon couplings, respectively. The first estimate of nEDM was based on the pion loop of the nucleon with the CP-violating π NN coupling \bar{g}_0 from the Ξ and nucleon mass difference [4] and from mixing with the Δ resonance [5]. These LECs can be obtained from baryon mass differences by comparing the \bar{g}_0 term with the expansion of the quark mass term, which is modified by the presence of the $\bar{\theta}$ term. The mass and CPV terms appear in the HB χ PT Lagrangian only at $O(p^2)$, and if the decuplet terms are neglected, the expansion of $\bar{\theta}$ in the modified mass $\chi = 2B(M + im^* \bar{\theta})$ in the mass coupling term gives

$$\bar{g}_0 = -\frac{(\Delta M_N)_{\text{QCD}}}{2F_\pi} \frac{m^* \bar{\theta}}{\bar{m} \epsilon} = -\frac{(\Delta M_N)_{\text{QCD}}}{2F_\pi} \left(\frac{1 - \epsilon^2}{2\epsilon} \right) \bar{\theta} + O\left(\frac{\bar{m}}{m_s}\right) \quad (11)$$

where $\bar{m} = \frac{m_u + m_d}{2}$, $\epsilon = \frac{m_d - m_u}{m_d + m_u}$ and $(\Delta M_N)_{\text{QCD}}$ is the neutron and proton mass difference in QCD, accounting for isospin breaking due to the different u and d quark masses without QED effects. While this leading-order result in Eq. (11) has been known for some time [4, 17, 21], it has been observed that considering the isospin splitting in $SU(3)$ χ PT to the next-to-next-leading order (N²LO), i.e., $O(m_q^2)$, the relation between ΔM_N and \bar{g}_0 holds to within a few percent [61]. Using lattice input for ΔM_N , m_u , and m_d [62, 63], a precisely determined \bar{g}_0 is obtained [61, 63]

$$\bar{g}_0 = -15.5 (2.0) (1.6) \times 10^{-3} \bar{\theta}. \quad (12)$$

This CPV π NN coupling can be obtained from the Schiff moments of nEDM and pEDM. It can also be determined from the pseudoscalar form factor in the nucleon in the presence of the θ term. Assuming pion dominance of the pseudoscalar form factor, \bar{g}_0 can be obtained from the matrix element

$$\langle N(p') | \bar{\psi} i \gamma_5 \psi (-i \bar{\theta} Q) | N(p) \rangle = \bar{u}(p') \bar{g}_P(q^2) u(p), \quad (13)$$

where q^2 is the momentum transfer. Assuming pion pole dominance, we have

$$\bar{g}_P(q^2) = \left(\frac{m_\pi^2 f_\pi}{2m_q} \right) \frac{\bar{g}_0}{-q^2 + m_\pi^2}. \quad (14)$$

A recent lattice calculation of the pseudoscalar form factor with the the topological charge insertion has been carried out [64] by the χ QCD collaboration based on the same ensemble of lattices used for the nEDM and pEDM calculation [42]. They obtained $\bar{g}_0 = -0.01713(62) \bar{\theta}$, which is consistent with the value in Eq. (12), and the statistic error is about 3 times smaller. Similar to Fig. 2, the pion mass dependence of \bar{g}_0 on the sea and valence pion masses is plotted in Fig. 3.

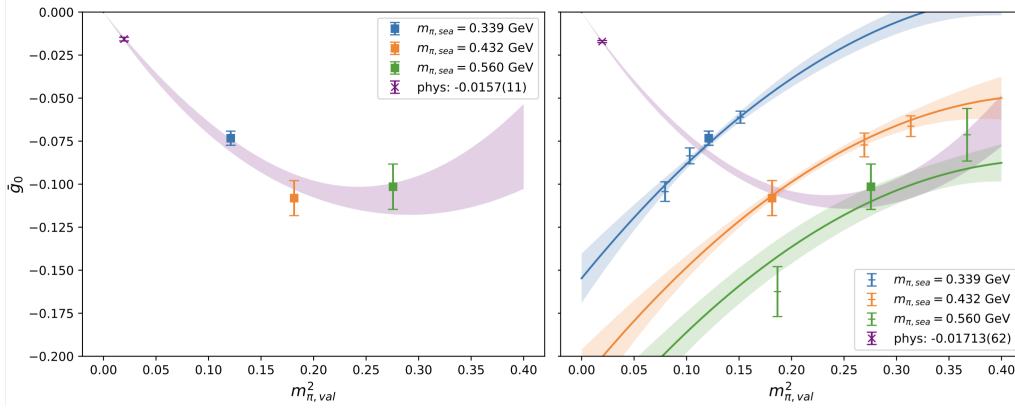


Figure 3: The same as in Fig. 2 for the CP-violating π NN coupling from the θ term. The left panel shows the unitary case, while the right panel presents the partially quenched results.

3. Weinberg operator

After integrating out heavy quarks and Higgs bosons, a dimension-6 CPV term emerges, specifically Weinberg's three-gluon operator [22].

$$O_W = k_W \text{Tr} ([G_{\mu\rho}, G_{\nu\rho}] \tilde{G}_{\mu\nu}). \quad (15)$$

The Weinberg operator can potentially contribute significantly to nEDM and pEDM since it is a pure glue operator. As such, it is not suppressed by small quark masses, unlike the θ term.

Calculating operators on the lattice requires renormalization, and dimension-6 operators can mix with lower dimensions operators, leading to power divergences in $1/a$. Given that the usual RI/MOM is an off-shell scheme with gauge fixing, the renormalization of the Weinberg's operator is complicated [65]. It mixes with three dimension-4 operators, and for $N_f \geq 3$, one dimension-5 operator. Additionally, it also mixes with thirty dimension-6 operators, twenty of which are 'nuisance' operators – some of which vanish with the equation of motion (EOM), while some others are gauge non-invariant. Although mixing with gauge-variant operators can be avoided by employing the background-field method [66], the remaining mixing patterns still present significant challenges for the numerical aspects of the lattice calculation.

An alternative to the RI/MOM scheme is gradient flow [44, 45, 67]. This is a gauge-invariant renormalized smoothing procedure that modifies the fields at short distances through a diffusion

equation. To explore where the power divergences have gone, it is useful to consider the short flow-time behavior of the composite operators.

The short flow-time expansion (SFTE) [68] of the gauge-invariant renormalized local operators $(O_i)_R(t)$ can be expanded as

$$(O_i)_R(t) \stackrel{t \rightarrow 0}{\sim} \sum_j c_{ij}(t) (O_j)_R(0), \quad (16)$$

where $(O_j)_R(0)$ are renormalized operators at $t = 0$ that have the same symmetry as (O_i) at t and dimensions that are equal to or lower than that of $(O_i)(t)$. The SFTE is an operator product expansion around $t = 0$, with Wilson coefficients $c_{ij}(t)$ that can be computed perturbatively. The flow-time dependence is encapsulated in these Wilson coefficients [68].

In lattice perturbation theory, there is only one scale — lattice spacing a — which serves the roles of both the cutoff and the renormalization scale. It is non-trivial to disentangle these roles, especially when the operator is mixed with lower dimensional ones, leading to power divergence in $1/a$. Gradient flow provides a solution by introducing a new scale in the flow time t , distinct from the lattice cutoff scale. In the continuum limit, all correlators are functions of the flow time with a scale $\mu^2 \propto 1/t$. The SFTE offers a method to extract renormalized operators at $t = 0$ and their mixings from operators calculated at $t > 0$ which are finite. The challenge associated with the renormalization of operators at finite a in other renormalization scheme is replaced by the determination of the Wilson coefficients $c_{ij}(t)$ in Eq. (16). One desirable feature here is that the analysis can be performed in the continuum, avoiding cumbersome chiral symmetry breaking effects associated with non-chiral fermion actions at finite a .

With the renormalized Weinberg operator in the flow defined as $O_G^R(x, t) := \frac{1}{g^2} \text{Tr}[G_{\mu\nu} G_{\nu\lambda} \tilde{G}_{\lambda\mu}]$, where g is the renormalized coupling and the gauge field-strength tensor defined in term of flowed gauge fields. The perturbative SFTE for the Weinberg operator has been calculated [69] for the mixing of lower-dimensional operator up to $O(g^2)$. To this order, only the topological charge term contributes

$$O_G^R(t) \stackrel{t \rightarrow 0}{\sim} -\frac{9\alpha_s C_A}{16\pi} \frac{1}{t} O_\theta^R(0) + \dots \quad (17)$$

Notably, there is a $1/t$ term, indicating that the Wilson coefficient diverges as $t \rightarrow 0$. This contrasts with the $1/a^2$ power divergence found in off-shell renormalization schemes, such as RI/MOM. The susceptibility of the Weinberg operator in the gradient flow exhibits a divergent behavior as t becomes small, in contrast to the flat behavior of topological susceptibility as a function of the flow time [70]. This aligns with the expected $1/t$ behavior of $O_G^R(t)$ in Eq. (17).

A preliminary lattice gradient flow calculation of F_3 using the Weinberg operator in place of the θ term has been attempted [71]. The calculations were conducted with clover valence fermions on multiple HISQ lattices with different lattice spacings and quark masses. This represents the raw lattice data at a fixed gradient flow time $t_{\text{gf}} \approx 0.34$ fm.

Completing the calculation is a challenging task, as it requires consideration of mixing with lower-dimensional operators exhibiting $1/t$ behavior, operators of same dimension with logarithmic t dependence, and higher dimension operators with $O(t)$ dependence. Furthermore, these mixed operators need to be renormalized at $t = 0$.

4. Quark electric dipole moment and quark chromoelectric dipole moment

At dimension 5, there are two CPV operators

$$\mathcal{L}_q^{\mathcal{CP}} = -\frac{i}{2} \sum_q d_q \bar{q} \sigma_{\mu\nu} \tilde{F}_{\mu\nu} q - \frac{i}{2} \sum_q \bar{d}_q \bar{q} \sigma_{\mu\nu} \tilde{G}_{\mu\nu} q, \quad (18)$$

where the first term represents the quark EDM (qEDM) with $\tilde{F}_{\mu\nu}$ being the dual of the electromagnetic field tensor $F_{\mu\nu}$ (note that $\sigma_{\mu\nu} \tilde{F}_{\mu\nu} = -\sigma_{\mu\nu} \gamma_5 F_{\mu\nu}$.) This entails the evaluation of the tensor charge of the nucleon, a task well-suited for lattice calculations. The tensor charge of the nucleon can be obtained from the nucleon matrix element of the tensor current

$$\langle N(p) | \bar{q} \sigma_{\mu\nu} q | N(p) \rangle = g_T^q \bar{u}(p) \sigma_{\mu\nu} u(p). \quad (19)$$

Here, g_T^q is the tensor charge for the quark flavor q . It represents the first Mellin moment of the collinear transversity parton distribution function (PDF) and can be extracted from the transversity parton distribution from deep inelastic scattering.

The first lattice calculation of the g_T^q for the u, d and s quarks, including all systematics, was performed by the PNDEME collaboration [72]. These calculations utilized valence clover fermions on $N_f = 2 + 1 + 1$ HISQ configurations. More precise results were updated [73] using 11 ensembles of configurations for the connected insertion and 7(6) ensembles for the strange (light) quarks in the disconnected insertion. A simultaneous fit in terms of the lattice spacing and the light-quark masses at the physical pion mass of 135 MeV, in the $\overline{\text{MS}}$ scheme at 2 GeV, gives [73, 74]

$$g_T^u = 0.784(28)(10), \quad g_T^d = -0.204(11)(10), \quad g_T^s = -0.0027(16) \quad (20)$$

The quark chromoelectric dipole moment (qcEDM) exhibits a similarly complicated renormalization pattern [75] as the Weinberg term. The SFTE in Eq. (16) for the qcEDM operator is given by:

$$(O_{\text{qCEDM}})_R(t) \stackrel{t \rightarrow 0}{\sim} c_{CP} P_R(0) + c_{Cq} (O_q)_R(0) + \dots, \quad (21)$$

which indicates mixing with the lower dimensional operators $P = k_P \bar{\psi} \gamma_5 \psi$ and $O_q = (k_q/4) \epsilon_{\mu\nu\alpha\beta} G_{\mu\nu}^a G_{\alpha\beta}^a$. The ellipsis (\dots) denotes mixing with same dimension 5 and higher dimensional operators.

The leading order in a perturbative calculation [76] yields:

$$\begin{aligned} O_C^R(t) \stackrel{t \rightarrow 0}{\sim} & 6ig^2 \frac{k_C}{k_P} \frac{C_2(F)}{(4\pi)^2} \left\{ \frac{1}{t} + p^2 \left[\log(2p^2 t) + \gamma_E - \frac{11}{4} \right] \right\} O_P^R(0) \\ & + 4ig^2 \frac{k_C}{k_q} \frac{m}{(4\pi)^2} [\log(2p^2 t) + \gamma_E - 1] O_q^R(0) + \dots \end{aligned} \quad (22)$$

The Wilson coefficient c_{CP} confirms the expectation that the leading small t contribution of $O_C^R(t)$ is given by the pseudoscalar density, with a leading $1/t$ divergence.

There have been preliminary attempts to calculate qcEDM on the lattice [30, 38, 77–79]. One such calculation was performed by the Stony Brook-BNL group [38] using a DWF lattices with a lattice spacing of $a = 0.1141(3)$ fm at the physical pion mass. This involved a direct four-point function calculation with the qcEDM operator insertion. Only the connected insertions were calculated for both the CP-odd and CP-even correlators. Fig. 4 presents the contributions of the

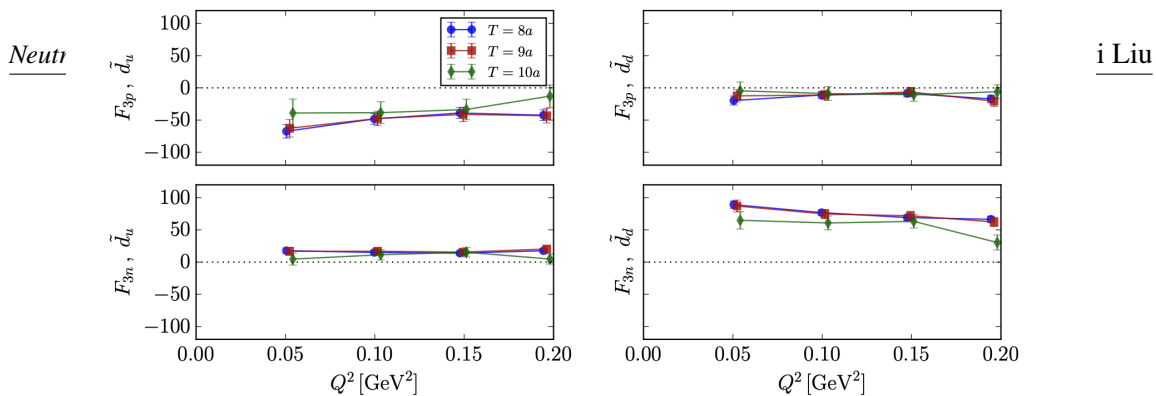


Figure 4: The contributions of the u and d quark to the bare F_3 form factors as functions of Q^2 for the neutron (n) and proton (p) are shown with different source-sink time separations T . The left panels display the contributions from the u quarks, while the right panels display those from the d quarks. This is a direct four-point function calculation with the qcEDM operator insertion [38].

u and d quark to the bare F_3 form factors for the neutron and proton at different source-sink time separation T . A crucial future plan for this approach will necessarily involve renormalization and mixing with operators of the same and lower dimensions in the RI-SMOM scheme [72].

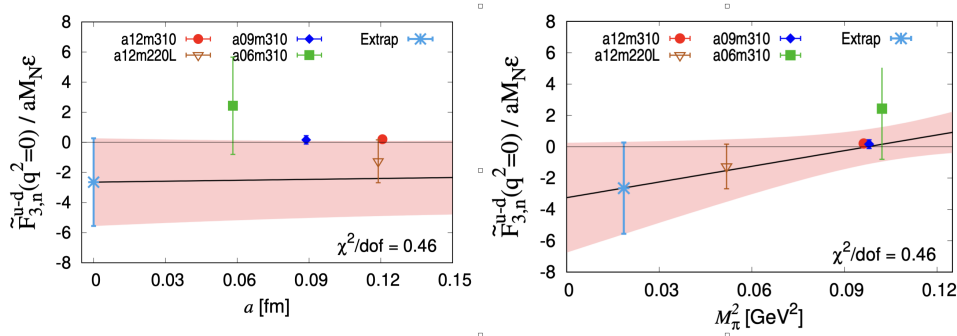


Figure 5: The simultaneous continuum (left) and chiral (right) extrapolations of the isovector nEDM, resulting from the qcEDM action, are calculated using the Schwinger source method [79].

Another recent qcEDM calculation was carried out by the Los Alamos group [79]. The calculation utilized clover fermions on four 2+1+1-flavor HISQ ensembles. Three of these ensembles have lattice spacings of $a = 0.12, 0.09$ and 0.06 fm, with a pion masses around 300 MeV. The fourth ensemble, also at $a = 0.12$ fm, has a pion mass at 227 MeV. These configurations were employed for continuum extrapolation and the study of pion mass dependence. They developed a Schwinger source method [77, 80] that incorporates the qcEDM operator, a quark bilinear, into the action to calculate the nucleon EDM. This involves reweighting the ratio of the determinants between the modified and the original ones. Additionally, the three-point function for the vector current must be calculated using a combination of quark propagators — with and without the qcEDM operator in the Dirac matrix — to examine the linear region of the small scale parameter multiplied by the qcEDM operator. Since this approach uses a mixed action with non-chiral valence fermions and the operators are not $O(a)$ improved, there is an $O(a)$ error [47]. The axial Ward identity

for the Wilson-clover action includes an additive term corresponding to the dimension-5 qcEDM operator [81–83]. Utilizing this identity, the isovector nEDM from the qcEDM is obtained for the power-divergence subtracted F_3 form factor, which is proportional to that from the pseudoscalar operator. However, it is found that the omitted $O(a^2)$ error can be as large as $\sim 25\%$ [79].

The results for the isovector neutron F_3 form factor at $q^2 = 0$ are shown in Fig. 5, with the continuum extrapolation presented in the left panel and m_π^2 dependence in the right panel. They obtained nEDM $F_3(0)/2M_N\epsilon = -2.6(2.9)$, where ϵ is the dimensionful parameter which multiplies the qcEDM term. The study also considered a fit accounting for the πN excited state contamination, which resulted in a 5-fold increase in $F_3(0)/2M_N\epsilon$.

The isovector case considered in this work allowed several simplifications: the determinant reweighting and the mixing with the topological term, and other dimension-5 operators are avoided. In the future when individual u, d, s quarks are considered, these complications need to be addressed [77].

5. Summary

Lattice QCD has matured to the point where it can calculate nucleon matrix elements with controlled systematic errors. We have observed significant improvements in the calculations of nEDM and pEDM with the θ term, despite the smallness of the signals. An important factor is the adoption of chiral fermions, which ensures that nEDM and pEDM are zero in the chiral limit at finite a . Additionally, variance reduction with the CEDR technique can decrease the variance of the signal by a volume factor. The agreement of the CP-violating πNN coupling from lattice calculations with predictions from the baryon spectrum serves as a consistency check between chiral perturbation theory and lattice calculations.

Lattice calculations of the Weinberg term and the quark chromo-electric dipole moment (qcEDM) have been undertaken. A major challenge for these operators is the complicated renormalization pattern. As higher dimensional operators, they mix with both other operators of the same dimension and lower-dimensional ones, leading to divergences in powers of $1/a$ in off-shell renormalization schemes, such as RI/MOM. The gradient flow with short flow-time expansion (SFTE) is gauge invariant and makes the renormalization of higher-dimensional operators more manageable. The power divergence of $1/a^2$ is reflected in the $1/t$ behavior in the SFTE as t approaches zero. In contrast to the small signal of nEDM due to the θ term, which is $\sim 10^{-3}$, the nEDM from the Weinberg term and qcEDM appear to be on the order of $O(1)$ to $O(10)$. This is encouraging news, indicating that the numerical efforts required to calculate these terms are less demanding.

Despite the statistical error of the current calculation of nEDM from the θ term is at the 10% level, it is based on chiral interpolation from heavier pion masses greater than 300 MeV. The calculation should be performed for ensembles at the physical pion mass, including systematic errors from continuum and infinite volume extrapolations.

ACKNOWLEDGMENTS

The author thanks T. Drape for reviewing the manuscript and J. Liang of χ QCD collaboration for providing the preliminary results on the CP-violating πNN coupling before publication. He

is grateful for discussions with K. Fuyuto, F. He, E. Mereghetti, A. Shindler, S. Syritsyn, and A. Walker-Loud. He is also indebted to P. Stoffer and Oscar Lara Crosas for pointing out the correct results and references for the renormalization of the Weinberg operator. This work is supported in part by the U.S. Department of Energy, Office of Science, Office of Nuclear Physics, under Grant No. DE-SC0013065. The author also acknowledges partial support by the U.S. Department of Energy, Office of Science, Office of Nuclear Physics under the umbrella of the Quark-Gluon Tomography (QGT) Topical Collaboration, with Award No. DE-SC0023646.

References

- [1] E. P. Shabalin. Electric Dipole Moment of Quark in a Gauge Theory with Left-Handed Currents. *Sov. J. Nucl. Phys.*, 28:75, 1978.
- [2] E. P. Shabalin. THE ELECTRIC DIPOLE MOMENT OF THE NEUTRON IN A GAUGE THEORY. *Sov. Phys. Usp.*, 26:297, 1983.
- [3] Chien-Yeah Seng. Reexamination of The Standard Model Nucleon Electric Dipole Moment. *Phys. Rev. C*, 91(2):025502, 2015.
- [4] R. J. Crewther, P. Di Vecchia, G. Veneziano, and Edward Witten. Chiral Estimate of the Electric Dipole Moment of the Neutron in Quantum Chromodynamics. *Phys. Lett. B*, 88:123, 1979. [Erratum: *Phys.Lett.B* 91, 487 (1980)].
- [5] Varouzhan Baluni. CP Violating Effects in QCD. *Phys. Rev. D*, 19:2227–2230, 1979.
- [6] R. D. Peccei and Helen R. Quinn. CP Conservation in the Presence of Instantons. *Phys. Rev. Lett.*, 38:1440–1443, 1977.
- [7] R. D. Peccei and Helen R. Quinn. Constraints Imposed by CP Conservation in the Presence of Instantons. *Phys. Rev. D*, 16:1791–1797, 1977.
- [8] Steven Weinberg. A New Light Boson? *Phys. Rev. Lett.*, 40:223–226, 1978.
- [9] Frank Wilczek. Problem of Strong P and T Invariance in the Presence of Instantons. *Phys. Rev. Lett.*, 40:279–282, 1978.
- [10] Stephen M. Barr and D. Seckel. Planck scale corrections to axion models. *Phys. Rev. D*, 46:539–549, 1992.
- [11] Marc Kamionkowski and John March-Russell. Planck scale physics and the Peccei-Quinn mechanism. *Phys. Lett. B*, 282:137–141, 1992.
- [12] Richard Holman, Stephen D. H. Hsu, Thomas W. Kephart, Edward W. Kolb, Richard Watkins, and Lawrence M. Widrow. Solutions to the strong CP problem in a world with gravity. *Phys. Lett. B*, 282:132–136, 1992.
- [13] S. Ghigna, Maurizio Lusignoli, and M. Roncadelli. Instability of the invisible axion. *Phys. Lett. B*, 283:278–281, 1992.

- [14] W. Buchmuller and D. Wyler. Effective Lagrangian Analysis of New Interactions and Flavor Conservation. *Nucl. Phys. B*, 268:621–653, 1986.
- [15] B. Grzadkowski, M. Iskrzynski, M. Misiak, and J. Rosiek. Dimension-Six Terms in the Standard Model Lagrangian. *JHEP*, 10:085, 2010.
- [16] Vincenzo Cirigliano and Michael J. Ramsey-Musolf. Low Energy Probes of Physics Beyond the Standard Model. *Prog. Part. Nucl. Phys.*, 71:2–20, 2013.
- [17] Jonathan Engel, Michael J. Ramsey-Musolf, and U. van Kolck. Electric Dipole Moments of Nucleons, Nuclei, and Atoms: The Standard Model and Beyond. *Prog. Part. Nucl. Phys.*, 71:21–74, 2013.
- [18] Elizabeth E. Jenkins, Aneesh V. Manohar, and Peter Stoffer. Low-Energy Effective Field Theory below the Electroweak Scale: Operators and Matching. *JHEP*, 03:016, 2018. [Erratum: *JHEP* 12, 043 (2023)].
- [19] Elizabeth E. Jenkins, Aneesh V. Manohar, and Peter Stoffer. Low-Energy Effective Field Theory below the Electroweak Scale: Anomalous Dimensions. *JHEP*, 01:084, 2018. [Erratum: *JHEP* 12, 042 (2023)].
- [20] Wouter Dekens and Peter Stoffer. Low-energy effective field theory below the electroweak scale: matching at one loop. *JHEP*, 10:197, 2019. [Erratum: *JHEP* 11, 148 (2022)].
- [21] J. de Vries, E. Mereghetti, R. G. E. Timmermans, and U. van Kolck. The Effective Chiral Lagrangian From Dimension-Six Parity and Time-Reversal Violation. *Annals Phys.*, 338:50–96, 2013.
- [22] Steven Weinberg. Larger Higgs Exchange Terms in the Neutron Electric Dipole Moment. *Phys. Rev. Lett.*, 63:2333, 1989.
- [23] Kenneth G. Wilson. Confinement of Quarks. *Phys. Rev. D*, 10:2445–2459, 1974.
- [24] David B. Kaplan. A Method for simulating chiral fermions on the lattice. *Phys. Lett. B*, 288:342–347, 1992.
- [25] Yigal Shamir. Chiral fermions from lattice boundaries. *Nucl. Phys. B*, 406:90–106, 1993.
- [26] Herbert Neuberger. Exactly massless quarks on the lattice. *Phys. Lett. B*, 417:141–144, 1998.
- [27] Peter Hasenfratz. Lattice QCD without tuning, mixing and current renormalization. *Nucl. Phys. B*, 525:401–409, 1998.
- [28] Andrea Shindler. Flavor-diagonal CP violation: the electric dipole moment. *Eur. Phys. J. A*, 57(4):128, 2021.
- [29] Keh-Fei Liu. Lattice QCD and the Neutron Electric Dipole Moment. *Ann. Rev. Nucl. Part. Sci.*, 75(1):377–397, 2025.

- [30] M. Abramczyk, S. Aoki, T. Blum, T. Izubuchi, H. Ohki, and S. Syritsyn. Lattice calculation of electric dipole moments and form factors of the nucleon. *Phys. Rev. D*, 96(1):014501, 2017.
- [31] E. Shintani, S. Aoki, N. Ishizuka, K. Kanaya, Y. Kikukawa, Y. Kuramashi, M. Okawa, Y. Taniguchi, A. Ukawa, and T. Yoshie. Neutron electric dipole moment from lattice QCD. *Phys. Rev. D*, 72:014504, 2005.
- [32] Keh-Fei Liu. Neutron Electric Dipole Moment at Fixed Topology. *Mod. Phys. Lett. A*, 24:1971–1982, 2009.
- [33] F. Berruto, T. Blum, K. Orginos, and A. Soni. Calculation of the neutron electric dipole moment with two dynamical flavors of domain wall fermions. *Phys. Rev.*, D73:054509, 2006.
- [34] F. K. Guo, R. Horsley, U. G. Meissner, Y. Nakamura, H. Perlt, P. E. L. Rakow, G. Schierholz, A. Schiller, and J. M. Zanotti. The electric dipole moment of the neutron from 2+1 flavor lattice QCD. *Phys. Rev. Lett.*, 115(6):062001, 2015.
- [35] Eigo Shintani, Thomas Blum, Taku Izubuchi, and Amarjit Soni. Neutron and proton electric dipole moments from $N_f = 2 + 1$ domain-wall fermion lattice QCD. *Phys. Rev.*, D93(9):094503, 2016.
- [36] C. Alexandrou, A. Athenodorou, M. Constantinou, K. Hadjiyiannakou, K. Jansen, G. Koutsou, K. Ottnad, and M. Petschlies. Neutron electric dipole moment using $N_f = 2 + 1 + 1$ twisted mass fermions. *Phys. Rev.*, D93(7):074503, 2016.
- [37] Keh-Fei Liu, Jian Liang, and Yi-Bo Yang. Variance Reduction and Cluster Decomposition. *Phys. Rev.*, D97(3):034507, 2018.
- [38] Sergey Syritsyn, Taku Izubuchi, and Hiroshi Ohki. Calculation of Nucleon Electric Dipole Moments Induced by Quark Chromo-Electric Dipole Moments and the QCD θ -term. *PoS, Confinement2018*:194, 2019.
- [39] Jack Dragos, Thomas Luu, Andrea Shindler, Jordy de Vries, and Ahmed Yousif. Confirming the Existence of the strong CP Problem in Lattice QCD with the Gradient Flow. *Phys. Rev. C*, 103(1):015202, 2021.
- [40] C. Alexandrou, A. Athenodorou, K. Hadjiyiannakou, and A. Todaro. Neutron electric dipole moment using lattice QCD simulations at the physical point. *Phys. Rev. D*, 103(5):054501, 2021.
- [41] Tanmoy Bhattacharya, Vincenzo Cirigliano, Rajan Gupta, Emanuele Mereghetti, and Boram Yoon. Contribution of the QCD Θ -term to the nucleon electric dipole moment. *Phys. Rev. D*, 103(11):114507, 2021.
- [42] Jian Liang, Andrei Alexandru, Terrence Draper, Keh-Fei Liu, Bigeng Wang, Gen Wang, and Yi-Bo Yang. Nucleon electric dipole moment from the θ term with lattice chiral fermions. *Phys. Rev. D*, 108(9):094512, 2023.

- [43] Fangcheng He, Michael Abramczyk, Tom Blum, Taku Izubuchi, Hiroshi Ohki, and Sergey Syritsyn. The calculations of Nucleon Electric Dipole Moment using background field on Lattice QCD. *PoS, LATTICE2023:336*, 2024.
- [44] Martin Lüscher. Properties and uses of the Wilson flow in lattice QCD. *JHEP*, 1008:071, 2010.
- [45] Martin Luscher. Chiral symmetry and the Yang–Mills gradient flow. *JHEP*, 1304:123, 2013.
- [46] Constantia Alexandrou, Andreas Athenodorou, Krzysztof Cichy, Martha Constantinou, Derek P. Horkel, Karl Jansen, Giannis Koutsou, and Conor Larkin. Topological susceptibility from twisted mass fermions using spectral projectors and the gradient flow. *Phys. Rev. D*, 97(7):074503, 2018.
- [47] Jiunn-Wei Chen, Donal O’Connell, and Andre Walker-Loud. Universality of mixed action extrapolation formulae. *JHEP*, 04:090, 2009.
- [48] Kazuo Fujikawa. A Continuum limit of the chiral Jacobian in lattice gauge theory. *Nucl. Phys. B*, 546:480–494, 1999.
- [49] David H. Adams. Axial anomaly and topological charge in lattice gauge theory with overlap Dirac operator. *Annals Phys.*, 296:131–151, 2002.
- [50] Jian Liang, Yi-Bo Yang, Terrence Draper, Ming Gong, and Keh-Fei Liu. Quark spins and Anomalous Ward Identity. *Phys. Rev. D*, 98(7):074505, 2018.
- [51] Yi-Bo Yang, Jian Liang, Yu-Jiang Bi, Ying Chen, Terrence Draper, Keh-Fei Liu, and Zhaofeng Liu. Proton Mass Decomposition from the QCD Energy Momentum Tensor. *Phys. Rev. Lett.*, 121(21):212001, 2018.
- [52] Jian Liang, Mingyang Sun, Yi-Bo Yang, Terrence Draper, and Keh-Fei Liu. Ratio of strange to u/d momentum fraction in disconnected insertions. *Phys. Rev. D*, 102(3):034514, 2020.
- [53] Gen Wang, Yi-Bo Yang, Jian Liang, Terrence Draper, and Keh-Fei Liu. Proton momentum and angular momentum decompositions with overlap fermions. *Phys. Rev. D*, 106(1):014512, 2022.
- [54] Bigeng Wang, Fangcheng He, Gen Wang, Terrence Draper, Jian Liang, Keh-Fei Liu, and Yi-Bo Yang. Trace anomaly form factors from lattice QCD. *Phys. Rev. D*, 109(9):094504, 2024.
- [55] Donal O’Connell and Martin J. Savage. Extrapolation formulas for neutron EDM calculations in lattice QCD. *Phys. Lett. B*, 633:319–324, 2006.
- [56] Terrence Draper, Nilmani Mathur, Jianbo Zhang, Andrei Alexandru, Ying Chen, Shao-Jing Dong, Ivan Horvath, Frank X. Lee, Keh-Fei Liu, and Sonali Tamhankar. On the Locality and Scaling of Overlap Fermions at Coarse Lattice Spacings. 9 2006.

- [57] Elizabeth Ellen Jenkins and Aneesh V. Manohar. Baryon chiral perturbation theory using a heavy fermion Lagrangian. *Phys. Lett. B*, 255:558–562, 1991.
- [58] E. Mereghetti, W. H. Hockings, and U. van Kolck. The Effective Chiral Lagrangian From the Theta Term. *Annals Phys.*, 325:2363–2409, 2010.
- [59] C. M. Maekawa, E. Mereghetti, J. de Vries, and U. van Kolck. The Time-Reversal- and Parity-Violating Nuclear Potential in Chiral Effective Theory. *Nucl. Phys. A*, 872:117–160, 2011.
- [60] J. Bsaisou, Ulf-G. Meißner, A. Nogga, and A. Wirzba. P- and T-Violating Lagrangians in Chiral Effective Field Theory and Nuclear Electric Dipole Moments. *Annals Phys.*, 359:317–370, 2015.
- [61] Jordy de Vries, Emanuele Mereghetti, and Andre Walker-Loud. Baryon mass splittings and strong CP violation in SU(3) Chiral Perturbation Theory. *Phys. Rev. C*, 92(4):045201, 2015.
- [62] Sz. Borsanyi et al. Ab initio calculation of the neutron-proton mass difference. *Science*, 347:1452–1455, 2015.
- [63] David A. Brantley, Balint Joo, Ekaterina V. Mastropas, Emanuele Mereghetti, Henry Monge-Camacho, Brian C. Tiburzi, and Andre Walker-Loud. Strong isospin violation and chiral logarithms in the baryon spectrum. 12 2016.
- [64] Jian Liang. pion NN coupling. private communication.
- [65] Vincenzo Cirigliano, Emanuele Mereghetti, and Peter Stoffer. Non-perturbative renormalization scheme for the CP -odd three-gluon operator. *JHEP*, 09:094, 2020.
- [66] L. F. Abbott. The Background Field Method Beyond One Loop. *Nucl. Phys. B*, 185:189–203, 1981.
- [67] R. Narayanan and H. Neuberger. Infinite N phase transitions in continuum Wilson loop operators. *JHEP*, 03:064, 2006.
- [68] Martin Lüscher. Future applications of the Yang-Mills gradient flow in lattice QCD. *PoS, LATTICE2013:016*, 2014.
- [69] Òscar L. Crosas, Christopher J. Monahan, Matthew D. Rizik, Andrea Shindler, and Peter Stoffer. One-loop matching of the CP-odd three-gluon operator to the gradient flow. *Phys. Lett. B*, 847:138301, 2023.
- [70] Jack Dragos, Thomas Luu, Andrea Shindler, and Jordy de Vries. Electric Dipole Moment Results from lattice QCD. *EPJ Web Conf.*, 175:06018, 2018.
- [71] Tanmoy Bhattacharya, Vincenzo Cirigliano, Rajan Gupta, Emanuele Mereghetti, and Boram Yoon. Calculation of neutron electric dipole moment due to the QCD topological term, Weinberg three-gluon operator and the quark chromoelectric moment. *PoS, LATTICE2021:567*, 2022.

- [72] Tanmoy Bhattacharya, Vincenzo Cirigliano, Rajan Gupta, Huey-Wen Lin, and Boram Yoon. Neutron Electric Dipole Moment and Tensor Charges from Lattice QCD. *Phys. Rev. Lett.*, 115(21):212002, 2015.
- [73] Rajan Gupta, Boram Yoon, Tanmoy Bhattacharya, Vincenzo Cirigliano, Yong-Chull Jang, and Huey-Wen Lin. Flavor diagonal tensor charges of the nucleon from (2+1+1)-flavor lattice QCD. *Phys. Rev. D*, 98(9):091501, 2018.
- [74] Y. Aoki et al. FLAG Review 2021. *Eur. Phys. J. C*, 82(10):869, 2022.
- [75] Tanmoy Bhattacharya, Vincenzo Cirigliano, Rajan Gupta, Emanuele Mereghetti, and Boram Yoon. Dimension-5 CP-odd operators: QCD mixing and renormalization. *Phys. Rev. D*, 92(11):114026, 2015.
- [76] Matthew D. Rizik, Christopher J. Monahan, and Andrea Shindler. Short flow-time coefficients of CP-violating operators. *Phys. Rev. D*, 102(3):034509, 2020.
- [77] Tanmoy Bhattacharya, Vincenzo Cirigliano, Rajan Gupta, Emanuele Mereghetti, and Boram Yoon. Neutron Electric Dipole Moment from quark Chromoelectric Dipole Moment. *PoS, LATTICE2015:238*, 2016.
- [78] Taku Izubuchi, Hiroshi Ohki, and Sergey Syritsyn. Computing Nucleon Electric Dipole Moment from lattice QCD. *PoS, LATTICE2019:290*, 2020.
- [79] Tanmoy Bhattacharya, Vincenzo Cirigliano, Rajan Gupta, Emanuele Mereghetti, Jun-Sik Yoo, and Boram Yoon. Quark chromoelectric dipole moment operator on the lattice. *Phys. Rev. D*, 108(7):074507, 2023.
- [80] Rajan Gupta, Tanmoy Bhattacharya, Vincenzo Cirigliano, and Boram Yoon. The Contribution of Novel CP Violating Operators to the nEDM using Lattice QCD. *EPJ Web Conf.*, 137:08007, 2017.
- [81] Luuk H. Karsten and Jan Smit. Lattice Fermions: Species Doubling, Chiral Invariance, and the Triangle Anomaly. *Nucl. Phys. B*, 183:103, 1981.
- [82] Marco Bochicchio, Luciano Maiani, Guido Martinelli, Gian Carlo Rossi, and Massimo Testa. Chiral Symmetry on the Lattice with Wilson Fermions. *Nucl. Phys. B*, 262:331, 1985.
- [83] D. Guadagnoli, V. Lubicz, G. Martinelli, and S. Simula. Neutron electric dipole moment on the lattice: A Theoretical reappraisal. *JHEP*, 04:019, 2003.